All-3d Electron-Hole Bilayers in CrN/MgO(111) Multilayers for Thermoelectric Applications

Antia S. Botana,[1] Victor Pardo,[2,3] and Warren E. Pickett[1]

[1]*Department of Physics, University of California Davis, Davis, California 95616, USA*
[2]*Departamento de Fisica Aplicada, Universidade de Santiago de Compostela,*
E-15782 Santiago de Compostela, Spain
[3]*Instituto de Investigacions Tecnoloxicas, Universidade de Santiago de Compostela,*
E-15782 Santiago de Compostela, Spain

CrN/MgO(111) multilayers modeled via *ab initio* calculations give rise to nanoscale, scalable, spatially separated two-dimensional electron and hole gases, each confined to its own CrN interface. Because of the Cr $3d^3$ configuration, both electron and hole gases are based on correlated transition-metal layers involving bands of $3d$ character. Transport calculations predict each subsystem will have a large thermopower, on the order of 250 μV/K at room temperature. These heterostructures combine a large thermoelectric efficiency with scalable nanoscale conducting sheets; for example, operating at a temperature difference of 50 K, 40 bilayers could produce a 1-V voltage with a film thickness of 100 nm.

I. BACKGROUND

The search for alternative functional materials that can be used in the fabrication of energy-recovery devices based on the thermoelectric (TE) effect has been a focus of interest [1–4]. The efficiency of TE devices at a given temperature can be evaluated by using the dimensionless figure of merit (*ZT*), defined as $ZT = S^2\sigma T/\kappa$, where S, T, σ, and κ are the Seebeck coefficient, the absolute temperature, the electrical conductivity, and the total thermal conductivity (electron and phonon contributions), respectively. Apparently, high *ZT* values can be achieved with concomitant high S and σ values, and low κ values. In standard systems, S, σ, and κ are interrelated, and the optimization of one often implies an undesired effect on the other; viz., a large S often occurs where σ is small.

Theoretical predictions suggesting that TE efficiency could be improved through nanostructural engineering reinvigorated interest in TE materials [5,6]. Using nanostructures is one possible strategy to optimize the magnitudes involved in *ZT* by reducing the lattice thermal conductivity κ. Based on density of states (DOS) considerations, a reduced dimensionality has a positive impact in the TE efficiency due to the increased TE power given by a narrow energy distribution of the electrons participating in the transport process [5,6]. Decoupling thermopower and electrical conductivity is also possible, with strain and nanostructuring being frequently suggested [7,8]. Following the reasoning based on nanoengineered systems, surface or interface states in thin-film geometries and multilayers have drawn attention recently. The observation [9] of a two-dimensional electron gas (2DEG) in LaAlO$_3$/SrTiO$_3$ (LAO/STO) interfaces has stimulated excitement for the design of similar heterostructures for a variety of reasons, including the enhancement of the TE power at the interface due to quantum confinement [9–14].

Recently, several authors have shown that transition-metal nitrides show a good TE response in addition to their excellent mechanical properties, thermal stability, ultra-hardness, and corrosion resistance [15–18]. As-grown bulk CrN exhibits a large TE power, reaching -185 μV/K at 420 K, an electrical resistivity that can be reduced through hole doping in the series Cr$_{1-x}$V$_x$N, keeping a large thermopower, and a relatively low thermal conductivity due to intrinsic lattice instabilities compared to other transition-metal nitrides. Overall, a *ZT* of 0.04 at room temperature can be achieved, still far from the value of *ZT* $\sim$ 1 usually required for applications. However, annealed thin films of epitaxial CrN(001) show a 250% increase of the figure of merit at room temperature, comparable to that of PbTe or SiGe alloys due to their much lower electrical resistivity while high thermopower values are retained [17]. These results, together with its excellent mechanical properties [19], make CrN a promising material for high-temperature TE applications.

In this paper, supported by first-principles and transport-property calculations, we propose enhancing the thermopower of nanoscale multilayers by making use of the favorable transport and mechanical properties of ionic nitrides, sandwiching CrN between, say, MgO layers along the rocksalt (111) direction. MgO is a widely used substrate material with a cubic rocksalt structure and a large band gap of 7.8 eV. MgO films with atomically flat (111) surface regions, and high-quality interfaces with other insulators have been reported using layer-by-layer growth on a variety of substrates, viz., GaN(0001), 6H-SiC(0001), Al$_2$O$_3$(0001), Ag(111), and SrTiO$_3$(111) [20–25]. Explanation of the growth of such strongly ionic layers and quality interfaces must confront the pioneering observations of Tasker [26]. Based on divergent lattice sums for an ideal semi-infinite crystal with a polar surface layer, he pointed out that such

surfaces must be unstable, and that substantial atomic reconstruction is one means to stabilize them. While layer-by-layer-grown interfaces do contain structural imperfections (see Ref. [27] for a recent discussion), interfaces with (111) orientation are reported to rival the more commonly studied (001) orientation in structural quality. The issue, of course, is the establishment of an internal electric field, for which there have been model [20,28–30] and first-principles [31,32] studies. We return to these questions in Sec. IV.

Considering that there are several reports of preparation of atomically flat MgO(111) surface areas, MgO is promising as a substrate to explore the possibility of polar interface engineering using mononitrides with a rocksalt structure. Bulk CrN is a paramagnetic semiconductor with a cubic rocksalt structure at room temperature that transforms to an antiferromagnet with orthorhombic structure below 285 K. The magnetic configuration consists of double ferromagnetic (FM) layers stacked antiferromagnetically along the [110] direction (AFM2) [33–35].

Recently, it was theoretically predicted [36] that ScN/MgO(111) multilayers designed as a superlattice constitute a different type of alternating metal-insulator multilayers with electron and hole 2DGs confined to the two opposing interfaces of the structure (beyond a critical thickness of ScN necessary for inducing interfacial metallicity). The ionic picture of CrN/MgO(111) multilayers is similar to the ScN case, leading to comparable polar distortions that give rise to alternating electron + hole conducting gases in subsequent interfaces but with an enhanced thermopower coming from the narrower Cr $3d$ bands around the Fermi level, which should also provide a large conductivity, particularly for the hole gas.

II. COMPUTATIONAL DETAILS

Electronic-structure calculations are performed within density-functional theory [37,38] using the all-electron, full-potential code WIEN2k [39] based on the augmented plane wave plus local orbitals basis set [40]. For the structural relaxations, we have used the Wu-Cohen version of the generalized gradient approximation (WC GGA) [41] that gives better lattice parameters for MgO than the Perdew-Burke-Ernzerhof functional does [42].

To deal with strong correlation effects, we apply the local-density approximation (LDA) + U scheme [43] that incorporates an on-site Coulomb repulsion U and Hund's rule coupling strength J_H for the Cr $3d$ states. The LDA + U scheme improves over GGA or LDA in the study of systems containing correlated electrons by introducing the on-site Coulomb repulsion U applied to localized electrons. The value $U = 4$ eV is used for CrN since it has been shown to give a reliable bulk spectrum [34,44] based on its agreement with photoemission experiments and transport properties, the comparison between band-structure parameters and optical data, and a comparison with parameter-free

functionals. The on-site Hund's exchange parameter is set as $J_H = 0.7$ eV. All calculations are well converged with respect to all of the parameters used. Specifically, we use $R_{mt}K_{max} = 7.0$, and the muffin-tin radii are 1.95 a.u. for Cr, 1.73 a.u. for N, 1.79 a.u. for Mg, and 1.69 a.u. for O. The calculations use a $43 \times 43 \times 5$ k-mesh for the integrations over the Brillouin zone. We model MgO/CrN(111) multilayers (1×1 in plane), with the thickness of the CrN block being varied from two to seven CrN layers. A barrier of four to five MgO layers (about 1 nm thick) between CrN blocks has been used for all of the calculations, checking that it is enough to guarantee the lack of interaction between the CrN blocks. AFM order along (111) is set in the CrN blocks. Note that the imposed AFM ordering along (111) is not the bulk CrN AFM2 ordering since it is not well adapted to the confinement constraint of these thin layers [33,35].

The in-plane lattice parameters are constrained to those of MgO (fixed to the cubic lattice constant 4.23 Å, obtained by optimizing the cell volume within WC GGA). The CrN grown on top of MgO is under tensile strain since its lattice parameter is approximately 2% smaller than that of MgO.

The transport properties are calculated using a semiclassical solution based on Bloch-Boltzmann transport theory within the constant scattering-time approximation by means of the BOLTZTRAP code [45], which uses the energy eigenvalues calculated by the WIEN2K code. The constant scattering-time approximation assumes that the energy dependence of the scattering time at a given temperature and doping level is negligible on the scale of $k_B T$. In this case, denser k meshes are required: in our case, up to $118 \times 118 \times 14$ to reach convergence.

III. RESULTS

A. Polar distortions

The (111) orientation of a rocksalt structure is polar, and a crystal cut along (111) presents alternating layers of metal and oxygen or nitrogen ions forming triangular sublattices in the a-b plane. The Cr and N planes have alternating formal charges 3^+ and 3^-, with 2^+ and 2^- for MgO (see Figs. 1 and 2). Hence, the heterostructure contains two charge-imbalanced interfaces (IFs): one n type (IFA, $2^-/3^+$) and one p type (IFB, $3^-/2^+$).

For all of the multilayers, we perform calculations with fully relaxed atomic positions also optimizing the value of the c-lattice parameter (off plane), i.e., allowing atomic displacements along the c axis and thus relaxing the interplane distances for the structures with different numbers of CrN layers. The optimized values of the c-lattice parameter result in a slight decrease from the value obtained by constructing the multilayers from the MgO bulk unit cell, of about 1% to 2% for multilayers two to seven CrN layers thick. This result is expected, as the in-plane lattice parameter inside the CrN blocks is constrained to that of MgO, which is larger (4.23 versus 4.13 Å for the cubic phase of CrN).
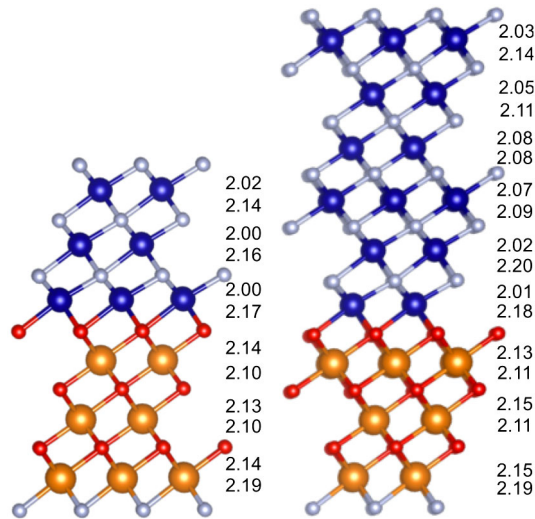
FIG. 1. Relaxed structure of MgO/CrN(111) multilayers three and six CrN layers thick, with Cr atoms in blue, N atoms in gray, Mg atoms in orange, and O atoms in red. The average distances between CrN layers along the z axis (in Å) are shown.

One of the main features in the calculated relaxed geometry is the presence of a considerable polar distortion along the (111) direction, with the atomic displacements being exclusively along the c axis. On the CrN side, they result in one shorter (2.01–2.07 Å) and one longer (2.14–2.18 Å) Cr—N or Cr—O bond length, as can be seen in Fig. 1. The distances are balanced in the inner layers for the thicker CrN blocks, somehow recovering the nearest-neighbor distance in bulk CrN of 2.07 Å. The distortions are also present on the MgO side, with Mg—O and Mg—N distances from 2.11 to 2.19 Å.

The polarity in MgO/CrN(111) multilayers gives rise to a large electrostatic potential offset between the two interfaces, proportional to the thickness of the CrN block.
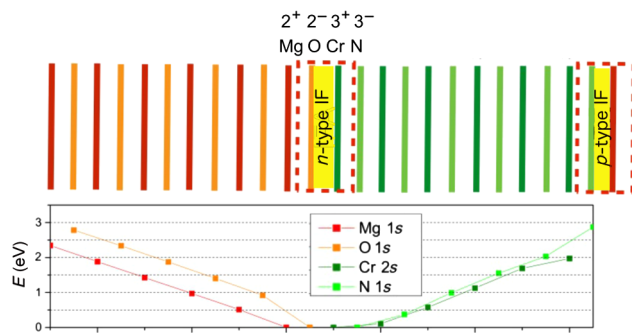

FIG. 2. (Top panel) Scheme showing the formal charge of the layers in a superlattice six CrN layers thick. 3^+ for Cr (dark green), 3^- for N (light green), 2^+ for Mg (red), and 2^- for O (orange). (Bottom panel) Potential gradient shown as the shift in the Mg/N/O $1s$ and Cr $2s$ core states layer by layer for a CrN/MgO(111) multilayer six CrN layers thick. The zero is set at IFA (n type). Cr $2s$ (dark green), N $1s$ (light green), Mg $1s$ (orange), and O $1s$ (red).

This internal potential can be tracked easily through the core levels, as shown in Fig. 2. A potential difference of 2 to 3 eV arises across the CrN and MgO slabs, increasing with an increasing thickness of the CrN block. The core level shifts are about 1 eV/layer in the thinner multilayer and are reduced as the CrN block becomes thicker. The fact that the inner layers of the thicker CrN slabs show no polar displacements (as discussed above) indicates that the internal electric field has been mitigated.

B. Electronic structure

The band gap of the system decreases with an increasing thickness of the CrN film before an insulator-to-metal transition takes place at four CrN layers, as a consequence of the potential gradient due to interface polarity. The transition between insulating and conducting states is hence a sharp function of the thickness, as is predicted and confirmed experimentally in LAO/STO heterostructures [46–48].

The density of states (DOS) for the case of a system three CrN layers thick (an insulating state) is depicted in Fig. 3(a). The electronic structure can be understood from a simple ionic picture: octahedral $Cr^{3+}: d^3$ with spin 3/2, and the e_g states at higher energy. The gap lies between occupied Cr(IFB) t_{2g} states and unoccupied Cr(IFA) e_g states. From the layer-by-layer DOS for the six CrN-layers case shown in Fig. 3(b), it is evident that the interfacial t_{2g} and e_g states are affected differently than the interior layers. Thus, the gap widening is better viewed as interface differentiation of the crystal field split Cr d states. The layer-by-layer shift from IFA to IFB (of 0.7 eV per Cr layer) arises from the internal electric field. Upon increasing the number of CrN layers, the gap between bands at IFA and IFB closes, with the insulator-to-metal transition occurring at a critical thickness of four CrN layers. When metallicity arises, the potential gradient is reduced significantly with respect to the thinner CrN layers due to a shift of electrons across the CrN slab. Band overlap of filled Cr t_{2g} bands at IFB with empty Cr e_g bands at IFA results in 2D bilayer conducting (hole + electron) gases, each confined to its own interface.

Figure 4 shows the band structures that complement Fig. 3 with a band character plot. The bands crossing the Fermi level are indeed Cr t_{2g} at IFB and Cr e_g at IFA. At the interface, the octahedral environment of the Cr atoms is clearly distorted, as can be observed in Fig. 1. Owing to the trigonal distortion, there is a splitting of the t_{2g} levels into a lower-lying e_g doublet and a higher-lying a_{1g} singlet. The a_{1g} band is flatter in character and gives rise to the 1D-like DOS. The e_g levels are unaffected by the trigonal distortion.

At first glance, the basic electronic structure seems similar to that of ScN/MgO multilayers. However, the states involved here at both interfaces are the much narrower Cr $3d$ bands, and this difference produces substantial enhancement of the TE response. Unlike other systems studied
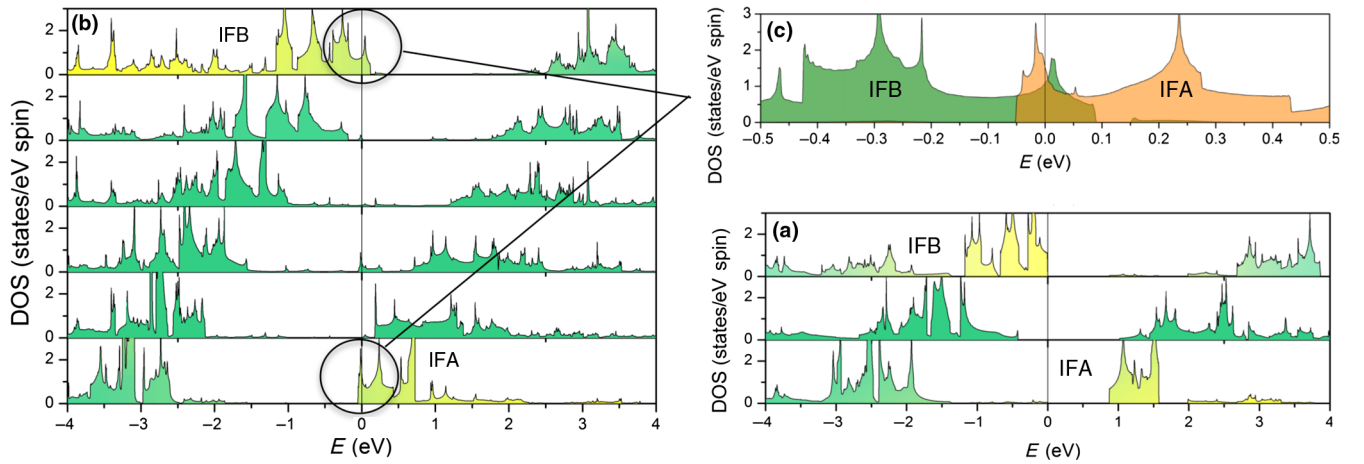
FIG. 3. Layer-resolved DOS for Cr atoms across the CrN slab from IFB to IFA for CrN/MgO(111) multilayers (a) three and (b) six CrN layers thick showing the Cr d states. The plots show the DOS for the majority spin. The shift in the Cr t_{2g} peak as moving from IFB to IFA can be observed. (c) Enlarged density of states around the Fermi level for a multilayer six CrN layers thick.

previously, the hole gas is formed by Cr $3d$ bands instead of N p bands or O p bands. The low (or zero) mobility of the holes at the p-type interface of LAO/STO multilayers leads to a negligible conductivity for that interface [48]. While the situation is improved in ScN/MgO(111) interfaces [36],
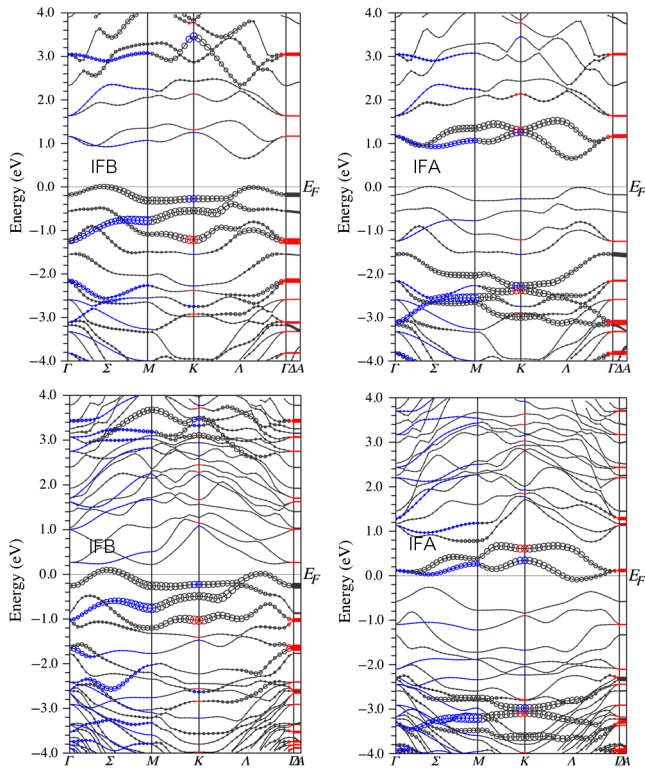

FIG. 4. Band structure with a band character plot for MgO/CrN(111) multilayers. (Right panels) Cr e_g at IFA and (left panels) Cr t_{2g} levels at IFB for CrN/MgO(111) multilayers (top panel) three and (bottom panel) six CrN layers thick.

CrN/MgO is qualitatively different due to the sole involvement of d-electron bands.

C. Transport properties

To check the TE response in this type of two-carrier 2DG multilayered system, we have carried out transport-property calculations based on Bloch-Boltzmann transport theory in the constant relaxation-time approximation. Within this approximation, the TE power is independent of the scattering time (τ). When a conventional two-carrier electron-hole system develops as in simple semimetals, hole and electron contributions to the Seebeck coefficient compensate, often resulting in a small, weakly temperature-dependent, and uninteresting thermopower. However, for these physically separated electron gases, it is appropriate and necessary to compute separately the contributions from each 2DG, i.e., from the electron pockets, then the hole pockets. The thermopower calculated from the semiclassical Bloch-Boltzmann expressions [49], which involve only Fermi-surface quantities, is shown in Fig. 5(a). Values of the TE power for electrons and holes are, accidentally, virtually identical in magnitude (both gases come from $3d$ electron bands of different symmetry), with the independent thermopower at each interface reaching very high values of about 250 μV/K above 300 K, where it becomes T independent. The DOS of electron and hole bands separately indicates that the enhanced thermopower comes from an almost 1D-like DOS arising at both interfaces [see Fig. 3(c)].

If one can complement this large thermopower with a large conductivity and a reduced thermal conductivity, this multilayered system can exhibit a TE performance comparable to that of the materials used in commercial TE devices. In our calculations within the constant relaxation-time approximation, σ/τ and κ/τ are obtained. Hence, the TE figure of merit ZT is independent of the scattering time
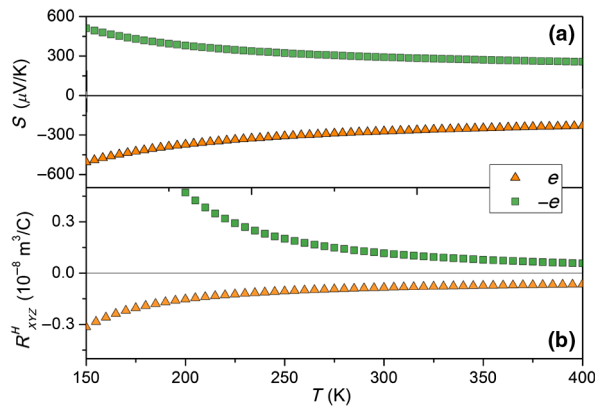
FIG. 5. Temperature dependence of (a) the in-plane thermopower and (b) the Hall coefficient for MgO/CrN multilayers six CrN layers thick for electrons and holes. The contributions to the net $S_{xx}(T)$ are discussed in the text. The calculations are done by summing over only the valence Fermi surfaces for the hole properties (green), only over the conduction Fermi surfaces for the electron properties (orange). At lower temperatures, $S(T)$ turns over and goes linearly to zero.
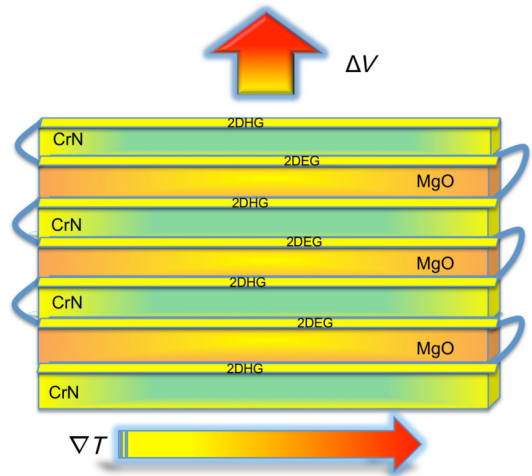

FIG. 6. Sketch of the thermoelectric module proposed using a nitride oxide platform consisting of parallel two-dimensional electron and hole gases (2DEG and 2DHG, respectively) created by interfacial confinement in a multilayered structure. The thermal gradient flows as shown, perpendicular to the voltage. The n- and p-type sectors are connected in series (with the wires represented pictorially), as usual in the type of thermoelectric module we describe in the text.

as the dependence on τ cancels out in σ/κ. It should be noted that this estimate contains the electronic contribution only since no phonon terms are considered for the thermal conductivity. Thus, it can be considered a theoretical upper limit of the figure of merit. The estimated ZT at room temperature for each 2DG separately is approximately 0.9 in the threshold required for applications. A more realistic estimate of the figure of merit for this system can be made using the TE power we have calculated, together with the experimental data for σ and κ taken from Ref. [17], giving rise to a value of 0.64 at room temperature.

The Hall coefficient is also τ independent within the constant relaxation-time approximation. The calculated values [see Fig. 5(b)] for electron- and holelike bands give $R_h^H = 0.06 \times 10^{-8}$ m^3/C, $R_e^H = -0.06 \times 10^{-8}$ m^3/C, both varying slowly with T above 300 K. Using a 2DG thickness of 3 Å, these values correspond in a standard parabolic single-band interpretation to an areal carrier density $n_e = n_h$ of 3.1×10^{14} carriers/cm^2. This value is similar in magnitude to the electronic density (from the Hall number) seen at the n-type LAO/STO interface at a large number of LAO overlayers [50,51].

IV. DISCUSSION AND SUMMARY

A. Some technical considerations

The parallel superlattice 2DEG + 2DHG of the type discussed here corresponds to alternately layered n- and p-type 2DGs, each with its own Hall voltage and Seebeck coefficient. This flexibility, plus the ability to vary the number of CrN layers in the heterostructure, provide a high degree of tunability that can be further controlled in a gate-voltage device. The large TE response that can be provided

by the two-carrier 2D gases independently makes this multilayered system promising as a TE device based on a nanoscale architecture. With $S(250 \text{ K}) = 250 \, \mu$V/K operating across a 50-K temperature difference, only 40 bilayers (as little as 100 nm) are necessary to create a 1-V voltage difference.

TE devices contain many TE couples consisting of n-type (electron carriers) and p-type (hole carriers) TE elements wired electrically in series and thermally in parallel. In the multilayered system proposed here, with the two gases showing a large TE response, one could envisage a TE module constructed as shown in Fig. 6, where each 2DG acts as the n- or p-type element of the TE couple. This scheme presents several intrinsic advantages for a nanoscale TE device. Such a device is intrinsically nanostructured, since the internal voltage scales with the nanostructuring of the device, and the n- and p-type parts can be isolated with just a 1- to 2-nm MgO barrier. The design proposed here would have very good compatibility between the n- and p-type materials (the match of electrical and thermal properties of the p- and n-type materials required for optimum efficiency of the TE device is often a challenging problem). Mechanical stability is another strong point of this nitride oxide system, and the scalability and nanoscale confinement of the 2DG can be controlled using atomic-force-microscopy lithography, enabling fabrication of nanoelectronic devices operating at the interface [12,13].

B. Growth of polar materials

Synthesis of the multilayers we have proposed requires the growth of charged layers a few nanometers thick.

Such growth at first appears daunting. Tasker established the widely known result that an ideal ionic surface of a semi-infinite polar crystal is unstable, based on the divergence of lattice sums [26]. Yet, as mentioned in the Introduction, several groups have established growth of charged (111) layers with interface quality that rivals that of neutral layers, based on transmission-electron microscopy and measured properties. Tasker proposed surface reconstruction (of the atomic geometry and, hence, the ionicity) as one means of stabilizing ionic surfaces [26]. The questions posed by observation of flat polar surfaces began to become more specific when Wander *et al.* made a theoretical investigation of ZnO(0001) surfaces [31]. There have since been several suggestions of ways to achieve flat polar nanostructures.

First, the semi-infinite geometry can be avoided. Growing (ultra)thin layers of the starting "substrate" has met with success. Matsuzaki and co-workers observed layer-by-layer growth of MgO(111) thin films on nonpolar NiO buffer layers up to ten MgO layers [23–25]. Only for thicker layers do step and terrace structures appear, presumably to counteract the growing dipole. Noguera and Goniakowski had performed model studies of such ultrathin films, concluding [28–30] that both surface (interface) charges and substantial lattice distortions can play a role in compensating for the electric dipole that increases with thickness. Surface or interface charges in MgO(111)/Ag(111) are also identified by Arita *et al.* as a mechanism of mitigating the increasing dipole in ultrathin MgO(111) films [32]. It had earlier been reported that unreconstructed wurtzite ZnO(0001) surfaces of thin films are assisted in stabilization by surface charges [31]. Surface composition and roughening during growth was identified by Benedetti *et al.* as a means to compensate for the growing dipole in MgO(111) films [52]. Different growth regimes can be accessed by control of the oxygen pressure, the growth temperature, and the availability of water vapor in the growth environment.

A key feature of the system we propose is that only alternating *ultrathin layers* of MgO and CrN are grown, and that the MgO(111) substrate can also be an ultrathin layer grown on a convenient nonpolar substrate. For the conducting interfaces that we envision, the metallic interface layers will provide a polarizability that will help to mitigate internal electric fields not only during growth but in the completed system as well. Finally, treatment of the uppermost surface may enhance stability of the atomic and electronic structure. The question of whether cations and anions can be grown to be sufficiently ordered (that is, with only minor intermixing) remains one for experiments to resolve.

C. Summary

To summarize, here we show an enhancement in the TE response in rocksalt nitride (CrN)/oxide (MgO)

superlattices grown along the polar (111) direction containing one *n*-type and one *p*-type interface. This multi-layered system has four distinctive features compared to the more highly studied multilayers. First, there is the (111) growth orientation, which very recently was shown to provide high-quality interfaces. Second, the d^3 configuration of the Cr ion dictates that both 2DGs have *d*-electron character: holes lie in the t_{2g} bands, with the electrons being promoted to the e_g bands. Third, both types of carriers lie in a transition metal *nitride* rather than oxide, which should provide high thermopower (on the order of 250 μV/K at room temperature) and a conductivity larger than common in oxides, particularly for the holes, which often localize at oxide interfaces. Finally, in a point that we have not emphasized, the carriers are fully spin polarized, with the magnetism being determined not by interface physics but by bulk properties, which will make it much more robust. It also raises the possibility of control of properties by a magnetic field, which is a topic for future study. Based on this configuration, we propose an alternative type of nanoscale TE device consisting of ultrathin nitride layers carrying electrons and holes at alternating interfaces. Such a device would provide significant advantages in terms of the improvement of standard losses and mechanical resistance issues, as well as a vast potential for scalability.

[1] F. J. D. Salvo, Thermoelectric cooling and power generation, Science **285,** 703 (1999).

[2] L. E. Bell, Cooling, heating, generating power, and recovering waste heat with thermoelectric systems, Science **321,** 1457 (2008).

[3] G. J. Snyder and E. S. Toberer, Complex thermoelectric materials, Nat. Mater. **7,** 105 (2008).

[4] J. P. Heremans, M. S. Dresselhaus, L. E. Bell, and D. T. Morelli, When thermoelectrics reached the nanoscale, Nat. Nanotechnol. **8,** 471 (2013).

[5] L. D. Hicks and M. S. Dresselhaus, Effect of quantum-well structures on the thermoelectric figure of merit, Phys. Rev. B **47,** 12727 (1993).

[6] J. O. Sofo and G. D. Mahan, Thermoelectric figure of merit of superlattices, Appl. Phys. Lett. **65,** 2690 (1994).

[7] P. L. Bach, J. M. Vila-Fungueiriño, V. Leboran, E. Ferreiro-Vila, B. Rodriguez-Gonzalez, and F. Rivadulla, Strain-induced enhancement of the thermoelectric power in thin films of hole-doped La$_2$NiO$_{4+\delta}$, APL Mater. **1,** 021101 (2013).

[8] V. Pardo, A. S. Botana, and D. Baldomir, Strain effects to optimize thermoelectric properties of hole-doped La$_2$NiO$_{4+\delta}$ via ab initio calculations, Phys. Rev. B **87,** 125148 (2013).

[9] A. Ohtomo and H. Hwang, A high-mobility electron gas at the LaAlO$_3$/SrTiO$_3$ heterointerface, Nature (London) **427,** 423 (2004).

[10] A. Filippetti, P. Delugas, M. J. Verstraete, I. Pallecchi, A. Gadaleta, D. Marré, D. F. Li, S. Gariglio, and V. Fiorentini, Thermopower in oxide heterostructures: The importance of being multiple-band conductors, Phys. Rev. B **86,** 195301 (2012).

[11] A. F. Santander-Syro, O. Copie, T. Kondo, F. Fortuna, S. Pailhs, R. Weht, X. G. Qiu, F. Bertran, A. Nicolaou, A. Taleb-Ibrahimi, P. L. Fvre, G. Herranz, M. Bibes, N. Reyren, Y. Apertet, P. Lecoeur, A. Barthlmy, and M. J. Rozenberg, Two-dimensional electron gas with universal subbands at the surface of SrTiO$_3$, Nature (London) **469,** 189 (2011).

[12] J. Mannhart and D. G. Schlom, Oxide interfaces–an opportunity for electronics, Science **327,** 1607 (2010).

[13] S. Park, D. H. Lee, J. Xu, B. Kim, S. W. Hong, U. Jeong, T. Xu, and T. P. Russell, Macroscopic 10-terabit-per-square-inch arrays from block copolymers with lateral order, Science **323,** 1030 (2009).

[14] P. Delugas, A. Filippetti, A. Gadaleta, I. Pallecchi, D. Marre, and V. Fiorentini, Large band offset as driving force of two-dimensional electron confinement: The case of SrTiO$_3$/SrZrO$_3$ interface, Phys. Rev. B **88,** 115304 (2013).

[15] S. Kerdsongpanya, B. Alling, and P. Eklund, Effect of point defects on the electronic density of states of ScN studied by first-principles calculations and implications for thermoelectric properties, Phys. Rev. B **86,** 195140 (2012).

[16] S. Kerdsongpanya, N. V. Nong, N. Pryds, A. Zukauskaite, J. Jensen, J. Birch, J. Lu, L. Hultman, G. Wingqvist, and P. Eklund, Anomalously high thermoelectric power factor in epitaxial ScN thin films, Appl. Phys. Lett. **99,** 232113 (2011).

[17] C. X. Quintela et al., Epitaxial CrN thin films with high thermoelectric figure of merit, Adv. Mater. **27,** 3032 (2015).

[18] C. X. Quintela, F. Rivadulla, and J. Rivas, Thermoelectric properties of stoichiometric and hole-doped CrN, Appl. Phys. Lett. **94,** 152103 (2009).

[19] F. Rivadulla, M. Banobre-Lopez, C. X. Quintela, A. Pineiro, V. Pardo, D. Baldomir, M. A. Lopez-Quintela, J. Rivas, C. A. Ramos, H. Salva, V. Pardo, J. S. Zhou, and J. B. Goodenough, Reduction of the bulk modulus at high pressure in CrN, Nat. Mater., **8,** 947 (2009).

[20] H. S. Craft, J. F. Ihlefeld, M. D. Losego, R. Collazo, Z. Sitar, and J.-P. Maria, MgO epitaxy on GaN (0002) surfaces by molecular beam epitaxy, Appl. Phys. Lett. **88,** 212906 (2006).

[21] T. L. Goodrich, J. Parisi, Z. Cai, and K. S. Ziemer, Low temperature growth of crystalline magnesium oxide on hexagonal silicon carbide (0001) by molecular beam epitaxy, Appl. Phys. Lett. **90,** 042910 (2007).

[22] A. Posadas, F. J. Walker, C. H. Ahn, T. L. Goodrich, Z. Cai, and K. S. Ziemer, Epitaxial MgO as an alternative gate dielectric for SiC transistor applications, Appl. Phys. Lett. **92,** 233511 (2008).

[23] T. Susaki, S. Kumada, T. Katase, K. Matsuzaki, M. Miyakawa, and H. Hosono, Fabrication of flat MgO(111) films on Al$_2$O$_3$(0001) substrates by pulsed laser deposition, Appl. Phys. Express **2,** 091403 (2009).

[24] K. Matsuzaki, H. Hosono, and T. Susaki, Layer-by-layer epitaxial growth of polar MgO(111) thin films, Phys. Rev. B **82,** 033408 (2010).

[25] K. Matsuzaki, H. Takagi, H. Hosono, and T. Susaki, Structural study of polar MgO(111) epitaxial thin films grown on SrTiO$_3$(111), Phys. Rev. B **84,** 235448 (2011).

[26] P. W. Tasker, The stability of ionic crystal surfaces, J. Phys. C **12,** 4977 (1979).

[27] H. Chen and A. Millis, Antisite defects at oxide interfaces, Phys. Rev. B **93,** 104111 (2016).

[28] J. Goniakowski, C. Noguera, and L. Giordano, Using Polarity for Engineering Oxide Nanostructures: Structural Phase Diagram in Free and Supported MgO(111) Ultrathin Films, Phys. Rev. Lett. **93,** 215702 (2004).

[29] J. Goniakowski, C. Noguera, and L. Giordano, Prediction of Uncompensated Polarity in Ultrathin Films, Phys. Rev. Lett. **98,** 205701 (2007).

[30] C. Noguera and J. Goniakowski, Polarity in oxide ultrathin films, J. Phys. Condens. Matter **20,** 264003 (2008).

[31] A. Wander, F. Schedin, P. Steadman, A. Norris, R. McGrath, T. S. Turner, G. Thornton, and N. M. Harrison, Stability of Polar Oxide Surfaces, Phys. Rev. Lett. **86,** 3811 (2001).

[32] R. Arita, Y. Tanida, S. Entani, M. Kiguchi, K. Saiki, and H. Aoki, Polar surface engineering in ultrathin MgO(111)/Ag(111): Possibility of a metal-insulator transition and magnetism, Phys. Rev. B **69,** 235423 (2004).

[33] A. S. Botana, V. Pardo, D. Baldomir, and P. Blaha, Conducting states caused by a surface electric dipole in CrN(001) very thin films, Phys. Rev. B **87,** 075114 (2013).

[34] A. S. Botana, F. Tran, V. Pardo, D. Baldomir, and P. Blaha, Electronic structure of CrN: A comparison between different exchange correlation potentials, Phys. Rev. B **85,** 235118 (2012).

[35] L. M. Corliss, N. Elliott, and J. M. Hastings, Antiferromagnetic structure of CrN, Phys. Rev. **117,** 929 (1960).

[36] A. S. Botana, V. Pardo, and W. E. Pickett, Nitride multilayers as a platform for parallel two-dimensional electron-hole gases: MgO/ScN(111), Phys. Rev. B **93,** 085125 (2016).

[37] P. Hohenberg and W. Kohn, Inhomogeneous electron gas, Phys. Rev. **136,** B864 (1964).

[38] R. O. Jones and O. Gunnarsson, The density functional formalism, its applications and prospects, Rev. Mod. Phys. **61,** 689 (1989).

[39] P. Blaha, K. Schwarz, G. K. H. Madsen, D. Kvasnicka, and J. Luitz, *WIEN2κ: An Augmented Plane Wave Plus Local Orbitals Program for Calculating Crystal Properties* (Vienna University of Technology, Vienna, 2001).

[40] E. Sjöstedt, L. Nördstrom, and D. Singh, An alternative way of linearizing the augmented plane-wave method, Solid State Commun. **114,** 15 (2000).

[41] Z. Wu and R. E. Cohen, More accurate generalized gradient approximation for solids, Phys. Rev. B **73,** 235116 (2006).

[42] F. Tran, R. Laskowski, P. Blaha, and K. Schwarz, Performance on molecules, surfaces, and solids of the Wu-Cohen GGA exchange-correlation energy functional, Phys. Rev. B **75,** 115131 (2007).

[43] A. I. Lichtenstein, V. I. Anisimov, and J. Zaanen, Density-functional theory and strong interactions: Orbital ordering in Mott-Hubbard insulators, Phys. Rev. B **52,** R5467(R) (1995).

[44] A. Herwadkar and W. R. L. Lambrecht, Electronic structure of CrN: A borderline Mott insulator, Phys. Rev. B **79,** 035125 (2009).

[45] G. K. Madsen and D. J. Singh, BOLTZTRAP: A code for calculating band-structure dependent quantities, Comput. Phys. Commun. **175,** 67 (2006).

[46] S. Thiel, G. Hammerl, A. Schmehl, C. W. Schneider, and J. Mannhart, Tunable quasi-two-dimensional electron gases in oxide heterostructures, Science **313,** 1942 (2006).

[47] R. Pentcheva and W. E. Pickett, Avoiding the Polarization Catastrophe in $LaAlO_3$ Overlayers on $SrTiO_3(001)$ through Polar Distortion, Phys. Rev. Lett. **102,** 107602 (2009).

[48] H. Chen, A. Kolpak, and S. Ismail-Beigi, First-principles study of electronic reconstructions of $LaAlO_3/SrTiO_3$ heterointerfaces and their variants, Phys. Rev. B **82,** 085430 (2010).

[49] P. B. Allen, W. E. Pickett, and H. Krakauer, Anisotropic normal-state transport properties predicted and analyzed for high-T_c oxide superconductors, Phys. Rev. B **37,** 7482 (1988).

[50] A. D. Caviglia, S. Gariglio, C. Cancellieri, B. Sacépé, A. Fête, N. Reyren, M. Gabay, A. F. Morpurgo, and J.-M. Triscone, Two-Dimensional Quantum Oscillations of the Conductance at $LaAlO_3/SrTiO_3$ Interfaces, Phys. Rev. Lett. **105,** 236802 (2010).

[51] R. Pentcheva, M. Huijben, K. Otte, W. E. Pickett, J. E. Kleibeuker, J. Huijben, H. Boschker, D. Kockmann, W. Siemons, G. Koster, H. J. W. Zandvliet, G. Rijnders, D. H. A. Blank, H. Hilgenkamp, and A. Brinkman, Parallel Electron-Hole Bilayer Conductivity from Electronic Interface Reconstruction, Phys. Rev. Lett. **104,** 166804 (2010).

[52] S. Benedetti, N. Nilius, P. Torelli, G. Renaud, H. J. Freund, and S. Valeri, Competition between polar and nonpolar growth of MgO thin films on Au(111), J. Phys. Chem. **115,** 23043 (2011).